*electronics*

MDPI

*Article*

# An Adaptive Controller with Disturbance Observer for Underwater Vehicle Manipulator Systems

**Xinhui Zheng [1,2,3,†], Yuliang Wang [1,2,3,†], Qiyan Tian [1,2,3,*], Qifeng Zhang [1,2,3], Xiaohui Wang [1,2,3], Wenbo Xu [1,2,3], Guodong Wang [1,2,3], Xuejiao Yang [1,2,3] and Yuze Sun [1,2,3]**

[1] State Key Laboratory of Robotics, Shenyang Institute of Automation, Chinese Academy of Sciences, Shenyang 110016, China; zhengxinhui@sia.cn (X.Z.); wangyuliang2@sia.cn (Y.W.); zqf@sia.cn (Q.Z.); wxh@sia.cn (X.W.); xubowen@sia.cn (W.X.); wangguodong@sia.cn (G.W.); yangxuejiao@sia.cn (X.Y.); sunyuze@sia.cn (Y.S.)
[2] Key Laboratory of Marine Robotics, Shenyang 110169, China
[3] University of Chinese Academy of Sciences, Beijing 100049, China
* Correspondence: tianqiyan@sia.cn
† These authors contributed equally to this work.

**Abstract:** Dynamic control of underwater vehicle manipulator systems (UVMSs) is the key part of underwater intervention tasks. In this paper, we propose an adaptive controller with a disturbance observer that mainly consists of two parts: the first part is the adaptive control law that estimates the changes in the center of mass (COM) and the center of buoyancy (COB) of the vehicle, and the second part is the nonlinear disturbance observer that estimates the external disturbance and model uncertainties. To attenuate the overestimation problem, a damping term is introduced to the adaptive law. The stability of the proposed method is proven on the basis of Lyapunov theory. We develop three scenarios on the Simurv platform and illustrate the effectiveness of the proposed method with a short response time and high tracking performance.

**Keywords:** UVMS; adaptive control; nonlinear disturbance observer; Simurv

check for updates

**Citation:** Zheng, X.; Wang, Y.; Tian, Q.; Zhang, Q.; Wang, X.; Xu, W.; Wang, G.; Yang, X.; Sun, Y. An Adaptive Controller with Disturbance Observer for Underwater Vehicle Manipulator Systems. *Electronics* **2024**, *13*, 3938. https://doi.org/10.3390/electronics13193938

Academic Editor: Dorin Petreus

Received: 20 August 2024
Revised: 27 September 2024
Accepted: 29 September 2024
Published: 5 October 2024

**Copyright:** © 2024 by the authors. Licensee MDPI, Basel, Switzerland. This article is an open access article distributed under the terms and conditions of the Creative Commons Attribution (CC BY) license (https://creativecommons.org/licenses/by/4.0/).

## 1. Introduction

Underwater vehicle manipulator systems (UVMSs) have been developed and widely used for performing underwater intervention tasks [1–5]. UVMSs are a combination of underwater vehicles and manipulators, and severe dynamic coupling torques exist because the movements of the manipulators affect control performance. Stable dynamic control is the key part of underwater intervention and has attracted widespread attention from researchers.

The most widely used control technique is proportional–integral–differential (PID) control [6]. The PID controller has the advantages of computational efficiency, fast convergence time and rapid response but cannot address nonlinear disturbances and higher-order systems. Thus, its performance severely decreases when a UVMS is facing water currents and dynamic coupling. The sliding mode control (SMC) technique inherits the advantages of the PID technique and guarantees state convergence [7–9], but the drawbacks of chattering are harmful to actuators. Fuzzy logic has been used for UVMS control and has achieved good results [10], but the development of a fuzzy logic system requires human experience. A neural network was used to obtain a desired action function [11] with a reinforcement learning framework. However, experimental datasets are difficult to obtain in the real world, and the simulations differ from those in the real world, which causes the famous sim2real gap problem [12].

The adaptive control technique was developed to enable a system to adapt to external payloads or disturbances and has been widely used for UVMS dynamic control. Mohan and Kim modeled the external disturbances as extended system states and proposed an

extended Kalman filter (EKF) to estimate the water current effects and model uncertainties [13]. Dai and Yu proposed an EKF to estimate the external disturbances and merged the disturbances into the control law for trajectory tracking of UVMS [14]. Yousefizadeh and Bak applied an EKF and a nonlinear disturbance observer to estimate the payloads of a manipulator [15]. Yang et al. combined an EKF and an adaptive control method to reject disturbances in low-resolution joint modules [16]. However, EKF-based methods require considerable computational effort and are less effective for UVMSs with limited computing resources. The other way is to design a simple adaptive law to realize exponential convergence of the estimated variables. In a seminal work, control of robot manipulators was achieved by estimating the inertia parameters via an adaptive law [17]. Then, an adaptive control scheme was applied to estimate the gravity parameters and ocean currents of underwater vehicles (UVs) [18]. A nonlinear disturbance observer was developed to estimate the model uncertainties, external disturbances and payloads in the manipulator system [19]. This technique estimates the system unknowns based on the nominal dynamic model. These two techniques are suitable for the dynamic control of UVMSs since accurate dynamic models are difficult to obtain.

Severe dynamic coupling occurs when UVMSs perform underwater intervention tasks; hence, the manipulators often move at slow and steady speeds, and the torques coupled to the vehicle are caused mainly by hydrostatic effects. Hydrostatic effects can be considered changes in the center of mass (COM) and center of buoyancy (COB) of the vehicle since the lean angle of the vehicle changes as the manipulators move. Moreover, UVMSs suffer severe time-varying external disturbances caused by water currents, which in turn decrease the intervention efficiency. To address these issues, an adaptive controller with a disturbance observer is developed to control the vehicle without any prior knowledge of the manipulators. First, we apply the adaptive control law to estimate the hydrostatic effects of the manipulators, which counter most of the disturbances of the vehicle. To avoid parameter overestimation when big initial errors exist in the system, we introduce a damping part to the adaptive law, and the damping term prevents further increase when the parameters are overestimated, which in turn guarantees the convergent speed of the parameters when only small errors exist. Then, with estimations of the hydrostatic effects, we design a nonlinear disturbance observer to estimate the time-varying external disturbances. The adaptive law estimates COM and COB positions changing, and provides more accurate system parameters to the disturbance observer. The observer then estimates the other disturbances and guarantees the tracking performance of the system.

The main contributions of this paper are summarized as follows:

- A sliding mode adaptive law is designed to estimate the COM and COB positions changing while the manipulator moves.
- A nonlinear disturbance observer is designed to estimate external disturbances and guarantees that the estimation errors converge.
- The stability of the proposed controller is guaranteed with parameter conditions.
- Various simulations are conducted and demonstrate the effectiveness of the proposed controller compared with a PID controller and an adaptive robust controller [20].

The rest of this paper is organized as follows. Section 2 describes the mathematical model of UVs. The proposed method is formulated in detail in Section 3. Simulations and discussions are given in Section 4. Section 5 presents the results of the research.

## 2. Mathematical Model

The mathematical model of underwater vehicles (UVs) in the body frame is [21,22]

$$M_v\dot{\nu} + C_v\nu + D_v\nu + g(\eta) = \tau_v + \tau_d \tag{1}$$

where $\eta = [x\ y\ z\ \phi\ \theta\ \psi]^T$ is the position and attitude vector of the vehicle in the inertia frame $\Sigma_I$, $\nu = [uvs.w\ p\ q\ r]^T$ is the velocity vector in the vehicle frame $\Sigma_V$, $M_v$ is the mass matrix including added terms, $C_v$ is the Coriolis matrix including added terms, $D_v$ is the

damping matrix, $g$ is the gravity and buoyancy vector, $\tau_v$ is the control input vector and $\tau_d$ is the external disturbance. Frame definitions of UVMS systems are shown in Figure 1.

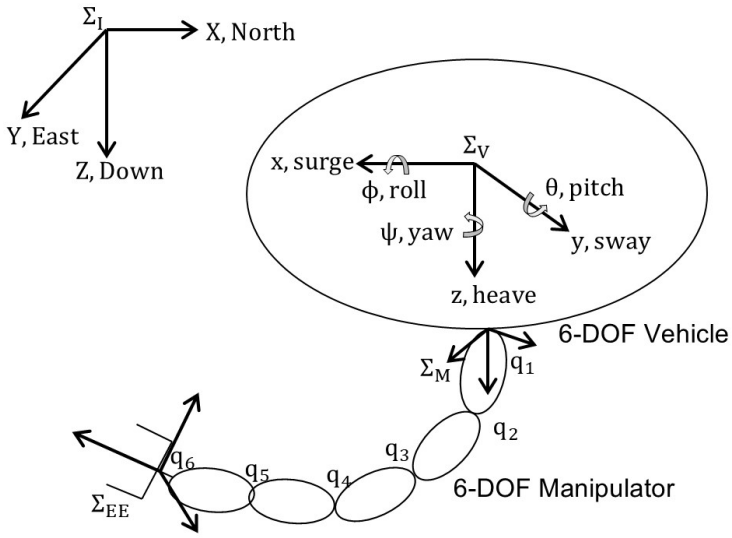


**Figure 1.** Frame definitions of UVMS systems. $\Sigma_I$ and $\Sigma_v$ are the inertia frame and body frame, respectively.

The coupling dynamics between the vehicle and the manipulator are considered as the forces and torques acting on the mounting point of the vehicle. The effects can be modeled as changes in the gravity vector.

Define $W$ and $B$ as the scalar gravity and buoyancy of the vehicle, $[x_g\ y_g, z_g]^T$ and $[x_b\ y_b, z_b]^T$ as the positions of the COM and COB in the body frame, $R_I^B$ as the rotation matrix from $\Sigma_I$ to $\Sigma_V$, $S(*)$ as the cross-product operator, and $p = [0\ 0\ 1]^T$ as a unit vector. The gravity and buoyancy vectors of the vehicle can be arranged as a linear expression with the $6 \times 4$ regressor matrix $\Phi_g$ and a grouped $4 \times 1$ gravity parameter $\Theta_g$ [22]

$$g = \Phi_g \Theta_g \tag{2}$$

where $\Phi_g = \begin{bmatrix} R_I^B p & 0_{3\times 3} \\ 0_{3\times 1} & S(R_I^B p) \end{bmatrix}$ and $\Theta_g = \begin{bmatrix} B - W \\ x_g W - x_b B \\ y_g W - y_b B \\ z_g W - z_b B \end{bmatrix}$.

Thus, the mathematical model of UVs with the parameterized gravity vector is

$$M_v \dot{\nu} + C_v \nu + D_v \nu + \Phi_g \Theta_g = \tau_v + \tau_d \tag{3}$$

## 3. Adaptive Controller with Disturbance Observer Design

In this section, we present the design process of the proposed adaptive controller with a disturbance observer. The basic idea is to combine the adaptive controller and the nonlinear disturbance observer, since the adaptive control law can estimate the movement of the COM and COB, which is caused by the movement of the manipulator, and the nonlinear disturbance observer can guarantee closed-loop stability. The proposed method consists of two main parts, as shown in Figure 2. The first part is the coupling estimation part with an adaptive control law, which estimates the gravity vector of UVs and provides a more accurate model for the nonlinear disturbance observer. The second part is a nonlinear disturbance observer that estimates uncompensated coupling effects, model uncertainties and external disturbances.

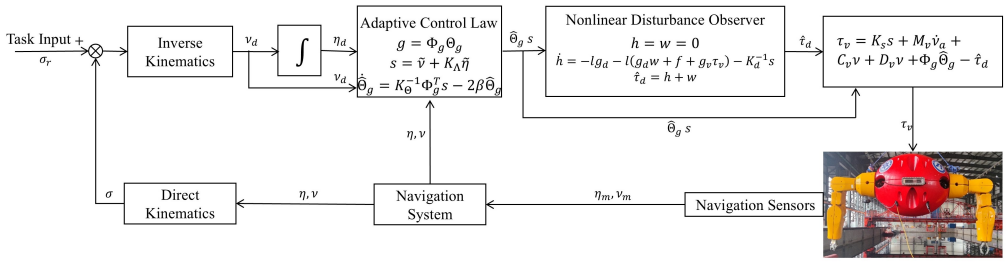


**Figure 2.** Flowchart of the proposed method. The inverse kinematics algorithm calculates the desired speed of the vehicle; then, the desired positions are calculated with velocity integrated over time. The adaptive law receives the desired values and calculates the sliding surface $s$ and $\hat{\Theta}_g$. The disturbance observer receives $\hat{\Theta}_g$ and $s$ and calculates the external disturbances $\hat{\tau}_d$. After all estimations are finished, the control law is calculated and sent to the vehicle.

### *3.1. Adaptive Control Law*

To avoid the attitude representation singularities of Euler angles, we use a unit quaternion to align the desired attitude and actual attitude. The quaternion of the desired frame is defined as $q_d = \{a_d, \epsilon_d\}$, and the quaternion of the current frame is defined as $q = \{a, \epsilon\}$, where $a$ and $\epsilon$ represent the scalar and vector parts of the unit quaternion, respectively.

Therefore, the quaternion error can be expressed as [23]

$$\tilde{a} = aa_d + \epsilon^T \epsilon_d \tag{4}$$

$$\tilde{\epsilon} = a\epsilon_d - a_d\epsilon + S(\epsilon_d)\epsilon \tag{5}$$

The velocity and position errors are defined as $\tilde{v} = v_d - v$ and $\tilde{\eta}_1 = \eta_{1,d} - \eta_1$. The sliding surface $s$ is defined as [17]

$$s = \tilde{v} + K_\Lambda \begin{bmatrix} R_I^B \tilde{\eta}_1 \\ \tilde{\epsilon} \end{bmatrix}$$

The control objective is then changed to $s = 0$, and the sliding surface guarantees that the position and attitude errors converge to zero exponentially.

The adaptive control law is

$$\tau_v = K_s s + M_v \dot{v}_a + C_v v + D_v v + \Phi_g \hat{\Theta}_g - \hat{\tau}_d \tag{6}$$

$$\dot{\hat{\Theta}}_g = K_\Theta^{-1} \Phi_g^T s - 2\beta \hat{\Theta}_g \tag{7}$$

where $v_a = v_d + K_\Lambda \begin{bmatrix} R_I^B \tilde{\eta}_1 \\ \tilde{\epsilon} \end{bmatrix}$ is the extended control input, $K_\Lambda$, $K_s$ and $K_\Theta$ are positive definite gain matrices, $\Phi_g$ is the regressor of the gravity vector, $\hat{\Theta}_g$ is the estimated parameter vector, $\beta$ is a scalar gain of $\hat{\Theta}_g$ and $\hat{\tau}_d$ is the estimated external disturbance.

The proposed control law (6) consists of a proportional part and a computed torque control (CTC) part, which are designed to guarantee fast convergence time and control accuracy. The CTC part requires an accurate dynamic model but is always difficult to derive in the real world. For UVMS systems, the total mass and volume of the system remain constant regardless of the configuration of the manipulator, and the coupling dynamics can be considered the movement of the COM and COB. Thus, the adaptive law (7) is designed. Different from the famous adaptive law [24], the adaptive law introduces a damping part $-2\beta\hat{\Theta}_g$ to slow the adaptive law integration and make the response speed of the system faster when the initial state is far from the desired state and $s$ is a large value. However, the excessively large parameter $\beta$ can lead to significant estimation errors. Thus, we can select large gains $K_\Theta^{-1}$ to speed up the integration to estimate large hydrodynamic effects and reduce estimation errors when the manipulator is heavy compared with the vehicle and $s$ fluctuates above and below 0. Regarding the external disturbances and model

uncertainties, a nonlinear disturbance observer is developed to estimate their effects, which is described in detail in the next subsection.

### *3.2. Nonlinear Disturbance Observer*

The coupling effects consist of hydrostatic effects and dynamic effects, and the former can be accurately estimated by the adaptive law. In addition, the adaptive law provides a more accurate estimation of the system, which further helps us to estimate the dynamic effects and external disturbances with the famous nonlinear disturbance observer [19].

In this paper, the dynamic effects and external disturbances are modeled as a union vector $\tau_d$, and a widely used assumption is made as follows.

**Assumption 1.** *The external disturbances $\tau_d$ are assumed to be bounded and slowly time-varying, and $\dot{\tau}_d = 0$ and $||\tau_d||^2 \leq \epsilon_d$ hold.*

To apply the famous nonlinear disturbance observer [19], Equation (3) can be rearranged to a more general form:

$$\dot{\nu} = -M_v^{-1}(C_v\nu + D_v\nu + \Phi_g\Theta_g) + M_v^{-1}\tau_v + M_v^{-1}\tau_d \tag{8}$$

$$\dot{\nu} = f(\nu) + g_v(\nu)\tau_v + g_d(\nu)\tau_d \tag{9}$$

where $f(\nu) = -M_v^{-1}(C_v\nu + D_v\nu + \Phi_g\Theta_g)$ and $g_v(\nu) = g_d(\nu) = M_v^{-1}$.

The nonlinear disturbance observer can be given as follows [19]:

$$\dot{h} = -l(\nu)g_d(\nu)h - l(\nu)(g_d(\nu)w + f(\nu) + g_v(\nu)\tau_v) - K_d^{-1}s \tag{10}$$

$$\hat{\tau}_d = h + w \tag{11}$$

where $h$, $w$ and $l$ are the inner variables and gains of the disturbance observer, and $K_d$ is the positive gain matrix of the sliding surface $s$. Different from the famous nonlinear observer [19], the revolution of the inner variables is related to the defined sliding surface $s$. The formulation $-K_d^{-1}s$ is introduced to the nonlinear disturbance observer as a cancel term to compensate for the effects to the system stability when the adaptive law is applied.

In our case, the inner variable $w$ is chosen as follows to simplify the observer calculation:

$$w = K_w\nu \tag{12}$$

where $K_w$ is a positive gain matrix.

With the definition of $w$, the following equation holds:

$$l(\nu) = \partial(w)/\partial(\nu) = K_w \tag{13}$$

To analyze the stability of the whole system, the time derivative of the estimated external disturbance vector $\hat{\tau}_d$ should be calculated with Assumption 1. The estimation error is defined as

$$\tilde{\tau}_d = \tau_d - \hat{\tau}_d$$

The time derivatives of the estimation errors can be derived as follows:

$$\begin{aligned}
\dot{\tilde{\tau}}_d &= 0 - \dot{\hat{\tau}}_d = -\dot{h} - \dot{w} \\
&= l(\nu)g_d(\nu)h + l(\nu)(g_d(\nu)w + f(\nu) + g_v(\nu)\tau_v) + K_d^{-1}s - l(\nu)\dot{\nu} \\
&= l(\nu)(g_d(\nu)(\hat{\tau}_d - w) + g_d(\nu)w + f(\nu) + g_v(\nu)\tau_v - \dot{\nu}) + K_d^{-1}s \\
&= l(\nu)(g_d(\nu)(\hat{\tau}_d - w) + g_d(\nu)w + f(\nu) + g_v(\nu)\tau_v - (f(\nu) + g_v(\nu)\tau_v + g_d(\nu)\tau_d)) + K_d^{-1}s \\
&= -l(\nu)g_d(\nu)\tilde{\tau}_d + K_d^{-1}s \\
&= -K_wM_v^{-1}\tilde{\tau}_d + K_d^{-1}s
\end{aligned} \tag{14}$$

where Equations (10)–(13) are used.

The time derivative of external disturbance errors is related to two parts: $-K_w M_v^{-1}\hat{\tau}_d$ and $-K_d^{-1}s$. The former introduces exponential stability of the external disturbances, and the latter introduces a cancel term to guarantee the overall system stability.

### *3.3. Stability Analysis*

In this section, we show the stability of the proposed control law. The positive Lyapunov candidate is defined as

$$V(t) = \frac{1}{2}s^T M_v s + \frac{1}{2}\tilde{\Theta}_g^T K_\Theta \tilde{\Theta}_g + \frac{1}{2}\tilde{\tau}_d^T K_d \tilde{\tau}_d$$

The time derivatives of the positive scalar function are

$$\dot{V} = s^T M_v \dot{s} + \tilde{\Theta}_g^T K_\Theta \dot{\tilde{\Theta}}_g + \tilde{\tau}_d^T K_d \dot{\tilde{\tau}}_d \tag{15}$$

Notably, the parameter $\Theta_g$ is bounded and slowly time-varying, and its time derivative is zero; then, $||\Theta_g||^2 \leq \epsilon_\Theta$ and $\dot{\tilde{\Theta}}_g = -\dot{\hat{\Theta}}_g$ hold, and $s$ and $\nu_a$ satisfy $s = \nu_a - \nu$.

Thus, substituting (3), (7) and (14) into (15), one obtains

$$\begin{aligned}
\dot{V} &= s^T(M_v\dot{\nu}_a - M_v\dot{\nu}) + \tilde{\Theta}_g^T K_\Theta \dot{\tilde{\Theta}}_g + \tilde{\tau}_d^T K_d \dot{\tilde{\tau}}_d \\
&= s^T(M_v\dot{\nu}_a + C_v\nu + D_v\nu + \Phi_g\Theta_g - \tau_d - \tau_v) + \tilde{\Theta}_g^T K_\Theta \dot{\tilde{\Theta}}_g + \tilde{\tau}_d^T K_d \dot{\tilde{\tau}}_d \\
&= s^T(M_v\dot{\nu}_a + C_v\nu + D_v\nu + \Phi_g\Theta_g - \tau_d - (K_s s + M_v\dot{\nu}_a + C_v\nu + D_v\nu \\
&\quad + \Phi_g\hat{\Theta}_g - \hat{\tau}_d)) + \tilde{\Theta}_g^T K_\Theta \dot{\tilde{\Theta}}_g + \tilde{\tau}_d^T K_d \dot{\tilde{\tau}}_d \\
&= -s^T K_s s + s^T\Phi_g\tilde{\Theta}_g - s^T\tilde{\tau}_d - \tilde{\Theta}_g^T K_\Theta \dot{\hat{\Theta}}_g - \tilde{\tau}_d^T K_d \dot{\tilde{\tau}}_d \\
&= -s^T K_s s + s^T\Phi_g\tilde{\Theta}_g - s^T\tilde{\tau}_d - \tilde{\Theta}_g^T K_\Theta (K_\Theta^{-1}\Phi_g^T s - 2\beta\hat{\Theta}_g) + \tilde{\tau}_d^T K_d(-K_w M_v^{-1}\tilde{\tau}_d + K_d^{-1}s) \\
&= -s^T K_s s - \tilde{\tau}_d^T K_d K_w M_v^{-1}\tilde{\tau}_d + 2\tilde{\Theta}_g^T K_\Theta \beta\hat{\Theta}_g \\
&= -s^T K_s s - \tilde{\tau}_d^T K_d K_w M_v^{-1}\tilde{\tau}_d + 2K_\Theta\beta((\tilde{\Theta}_g + \hat{\Theta}_g)^2 - \tilde{\Theta}_g^2 - \hat{\Theta}_g^2) \\
&\leq -s^T K_s s - \tilde{\tau}_d^T K_d K_w M_v^{-1}\tilde{\tau}_d - \tilde{\Theta}_g^\top (2K_\Theta\beta)\tilde{\Theta}_g + 2K_\Theta\beta\Theta_g^2 \\
&\leq -s^T K_s s - \tilde{\tau}_d^T K_d K_w M_v^{-1}\tilde{\tau}_d - \tilde{\Theta}_g^\top (2K_\Theta\beta)\tilde{\Theta}_g + 2\beta\lambda_{max}(K_\Theta)\epsilon_\Theta
\end{aligned} \tag{16}$$

where $\lambda_{max}(*)$ is the maximum eigenvalue operator.

The Lyapunov candidate is a bounded continuous positive scalar function, the first time derivative exists, its time derivative is negative if the following equation holds and the controller is asymptotically stable.

$$\lambda_{min}\left(\left\|\begin{bmatrix} s \\ \hat{\tau}_d \\ \tilde{\Theta}_g \end{bmatrix}\right\|^2 \begin{bmatrix} \frac{K_s}{2\beta\lambda_{max}(K_\Theta)\epsilon_\Theta} & 0 & 0 \\ 0 & \frac{K_d K_w M_v^{-1}}{2\beta\lambda_{max}(K_\Theta)\epsilon_\Theta} & 0 \\ 0 & 0 & \frac{K_\Theta}{\lambda_{max}(K_\Theta)\epsilon_\Theta} \end{bmatrix} - I_{13}\right) > 0 \tag{17}$$

where $\lambda_{min}(*)$ is the minimum eigenvalue operator.

The stability is related to the initial state of the system because of the positive bounds. $K_s$, $K_d$, $K_w$ and $K_\Theta$ are the main parameters related to the system convergence speed and are as large as possible to gain fast convergent performance. Furthermore, the scalar gain $\beta$ is the key factor of the system stability (i.e., if $\beta = 0$ then $\dot{V} \leq 0$ with any other parameters); however, to attenuate the overestimation problem, $\beta$ should select large values, and these parameters should guarantee Equation (17) to ensure system stability.

## 4. Simulations and Analysis

The simulations are conducted on the MATLAB and Simurv platforms [25], as shown in Figure 3. Simurv was developed for UVMS simulations in both kinematics and dynamics; it is not only a simulation platform but also a useful function library that provides coordinate transformation, Jacobin calculations, possible task functions, inverse dynamics and vehicle models. We tested the proposed method on the Simurv platform. The mathematical

models of the vehicle and the manipulator, which are widely used to develop control strategies, can be found in [26].

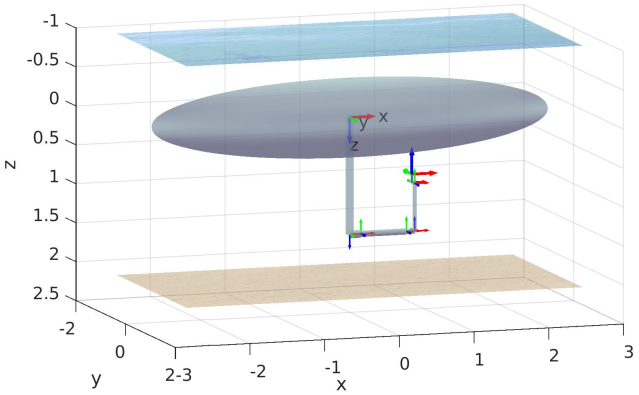


**Figure 3.** Simurv platform.

To verify the robustness of the proposed method, the mass matrix of the vehicle is assumed to be 90% of the real values in the calculation process (i.e., $M_v^* = 0.9M_v$). In addition, the Coriolis matrix and damping matrix are both omitted in the calculation process.

For comparison, a PID controller is added to the simulations, which is given as

$$\tau_v = K_1 e + K_2 \int e dt + K_3 \dot{e} \tag{18}$$

where $e$ is the vehicle control error, and $K_1$, $K_2$ and $K_3$ are positive control gain matrices.

An adaptive robust controller is added to the simulations [20], which is given as

$$\nu_d = \tilde{v} + R^{-1}\dot{\eta}_d + K_4 R^{-1}\tilde{\eta} \tag{19}$$

$$\tau_v = K_5 \tilde{v} + M_v \dot{\tilde{v}} + b \tag{20}$$

$$\dot{b} = \tilde{v} \tag{21}$$

where $K_4$ and $K_5$ are positive gain matrices, $R$ is the corresponding Jacobian matrix and $b$ is the estimated disturbance vector.

A sliding mode controller is added to the simulations, which is given as

$$\tau_v = M_v(K_6 s_2 + K_7 sign(s_2)) + C_v \nu + D_v \nu + g(\eta) \tag{22}$$

where $s_2 = \tilde{v} + \lambda_s \tilde{\eta}$ is the defined sliding surface, $sign(*)$ is the sign function $\lambda_s$ and $K_6$ and $K_7$ are positive gain matrices.

The joints are activated by a PID control law, which is given as

$$\tau_q = K_{pq} q_e + K_{iq} \int q_e dt + K_{dq} \dot{q}_e \tag{23}$$

where $q_e$ is the joint control error, and $K_{pq}$, $K_{iq}$ and $K_{dq}$ are positive control gain matrices.

We tuned the control parameters via trial and error. The control parameters of the proposed method are $K_\Lambda = diag(I_{3\times3}\ 10I_{3\times3})$, $K_s = 2000I_{6\times6}$, $K_\Theta^{-1} = 50I_{4\times4}$, $K_d = 5I_{6\times6}$ and $K_w = 10^4 diag(I_{3\times3}\ 0.5I_{3\times3})$. The control parameters of the PID controller of the vehicle are $K_1 = 2000diag(3I_{4\times4}\ 5I_{2\times2})$, $K_2 = 5000diag(I_{4\times4}\ 3I_{2\times2})$ and $K_3 = 200I_{6\times6}$. The control parameters of the adaptive robust controller of the vehicle are $K_4 = 0.1I_{6\times6}$ and $K_5 = 1000I_{6\times6}$. The control parameters of the sliding mode controller of the vehicle are $\lambda_s = diag(0.5I_{3\times3}\ 10I_{3\times3})$, $K_6 = diag(0.5I_{3\times3}\ I_{3\times3})$ and $K_7 = 0.01I_{6\times6}$. The control parameters of the PID controller of the manipulator are $K_{pq} = 200diag(10I_{3\times3}\ I_{3\times3})$, $K_{iq} = I_{6\times6}$ and $K_{dq} = 100diag(5I_{3\times3}\ 2I_{3\times3})$. The time step of the simulations is $0.01s$.

Three scenarios are designed to verify the effectiveness of the proposed method compared with that of the PID controller and adaptive robust controller. The first scenario is the conventional dynamic positioning (DP) task, which involves maintaining the attitude of the vehicle during the reciprocating motion of two joints of the manipulator. UVMSs often retain their position and perform intervention tasks; hence, the coupling torques in the system affect the attitude control and the gripper position control. The first scenario is designed to test the attitude control performance while considering severe dynamic coupling torques. The second scenario involves trajectory tracking while maintaining a desired attitude. For floating-base manipulation, the vehicle is always controlled to follow the desired trajectories. Thus, the second scenario is designed to test the position tracking performance while considering severe dynamic coupling torques. The second scenario consists of two parts: the first part tracks the desired trajectory, and the second part retains its position. The desired vehicle trajectory is governed by

$$\eta_d = \begin{bmatrix} 1sin(2\pi \times 0.03t), t \leq 25 \\ 1.5sin(2\pi \times 0.02t), t \leq 25 \\ 2sin(2\pi \times 0.01t), t \leq 25 \\ 0 \\ 0 \\ \frac{1}{9}\pi \end{bmatrix} \tag{24}$$

In these two scenarios, the joint trajectory of the six-degree-of-freedom (DOF) manipulator is governed by

$$q_d = \begin{bmatrix} 0 \\ \frac{2}{3}\pi sin(2\pi \times 0.1t) \\ \pi sin(2\pi \times 0.2t) \\ 0 \end{bmatrix} \tag{25}$$

The third scenario involves tracking the desired sinusoidal position trajectory of the tip link of the manipulator while maintaining the attitude of the vehicle. This scenario is a verification scenario to showcase the performance of different controllers in underwater intervention tasks. The desired tip link trajectory is governed by

$$\eta_{ee,d} = \begin{bmatrix} 1sin(2\pi \times 0.025t) \\ 1.5sin(2\pi \times 0.02t) \\ 0.5 + 0.5sin(2\pi \times 0.033t) \end{bmatrix} \tag{26}$$

Considering the sea environment, we add nonlinear irrotational water currents to Scenarios 2 and 3, which are governed by (27). The water currents are modeled as the relative velocity of the vehicle [21], and and the water currents are governed by

$$\nu_c = \begin{bmatrix} 0.3sin(2\pi \times 0.1t + 1) \\ 0.1sin(2\pi \times 0.1t + 3) \\ 0.5sin(2\pi \times 0.1t + 5) \\ 0 \\ 0 \\ 0 \end{bmatrix} \tag{27}$$

For comparisons among the three types of controllers, we calculate eight performance indices, $J_1$ to $J_8$. They are calculated by

$$J_1 = \int_0^{50} e_x dt,\ J_2 = \int_0^{50} e_y dt,\ J_3 = \int_0^{50} e_z dt,\ J_4 = \int_0^{50} e_\phi dt,\ J_5 = \int_0^{50} e_\theta dt,\ J_6 = \int_0^{50} e_\psi dt$$

$$J_7 = max||\tilde{\eta}_1||^2,\ J_8 = \int_0^{50} \tau_v dt$$

where $e_x$,$e_y$,$e_z$,$e_\phi$,$e_\theta$,$e_\psi$ are abstract values of position tracking errors in 6DOF.

The tracking history of Scenario 1 is shown in Figure 4, and the related performance indices are given in Table 1. The performance of SMC, Robust and Proposed controllers are satisfactory for all degrees, whereas that of the PID controller is the worst. The total linear tracking error of the PID controller in the $z$ direction is 11.3 ms because of the existing buoyancy of the vehicle, whereas it is 5.6 ms 4.0 ms and 4.9 ms with SMC, Robust and Proposed methods. Moreover, the attitude performance indices of the two controllers are also smaller than those of the PID controller. The total pitch tracking error of the PID controller is 3.0 rads since the movement of the manipulator affects the pitch control of the vehicle. The other three controllers perform well because they can adapt to the system's COM and COB positions changing and achieve better control performance. In these controllers, the proposed controller shows the best position-holding performance in all directions, even though the Robust controller can estimate the external disturbances online. However, the estimated parameters reach to the extended value in 5 s, so the parameters are overestimated. The overestimation problem occurs because the desired system state is far from the current system state. The adaptive parameter history is shown in Figure 5. In addition, the energy consumption of the proposed method is not the smallest. The actuator of the proposed method is saturated because of the large initial state errors, and thus the energy consumption is higher compared with the adaptive robust controller. In this scenario, despite the higher energy consumption, the proposed method performs well on the DP task with a short response time and small tracking errors.

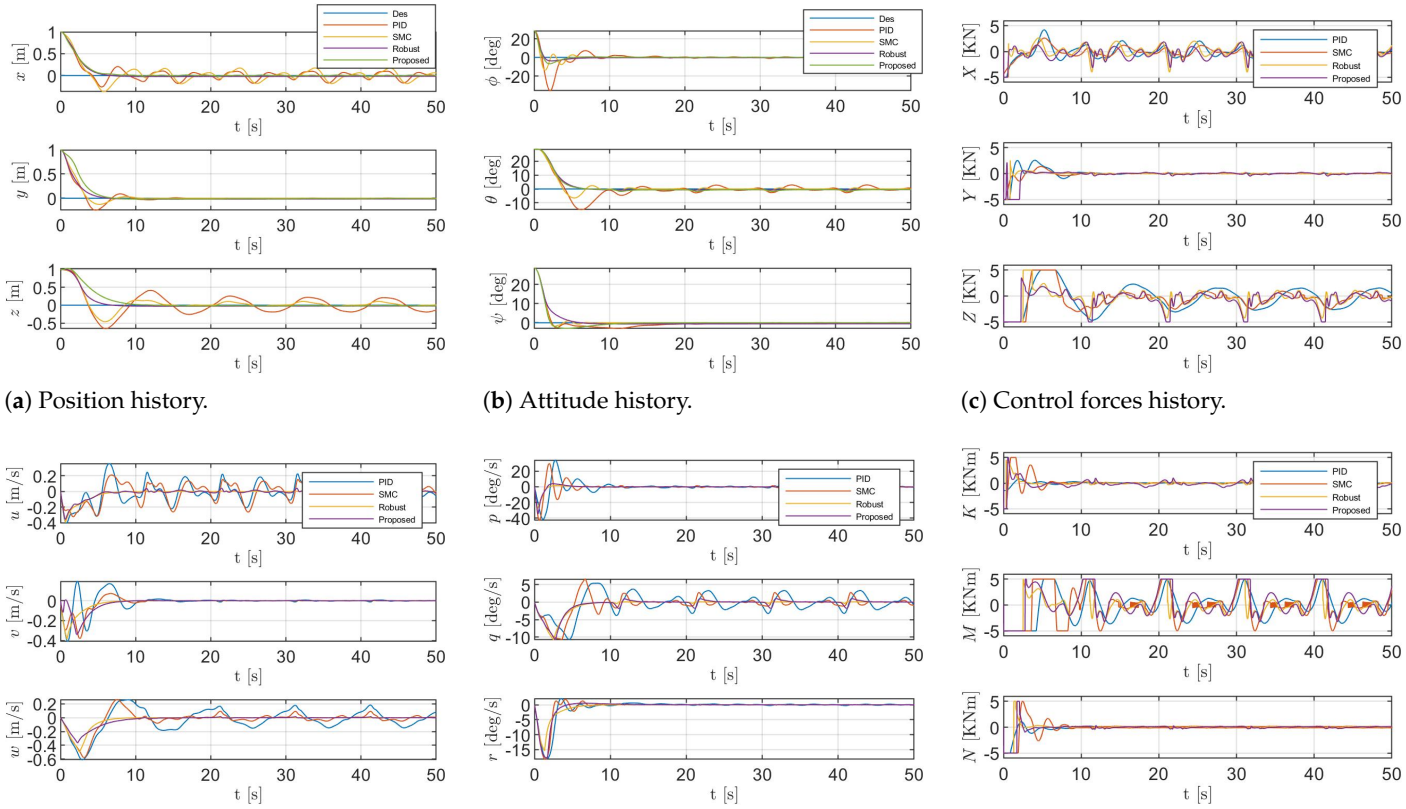


(**a**) Position history. (**b**) Attitude history. (**c**) Control forces history.

(**d**) Linear velocity history. (**e**) Angular velocity history. (**f**) Control torques history.

**Figure 4.** Tracking history of Scenario 1.

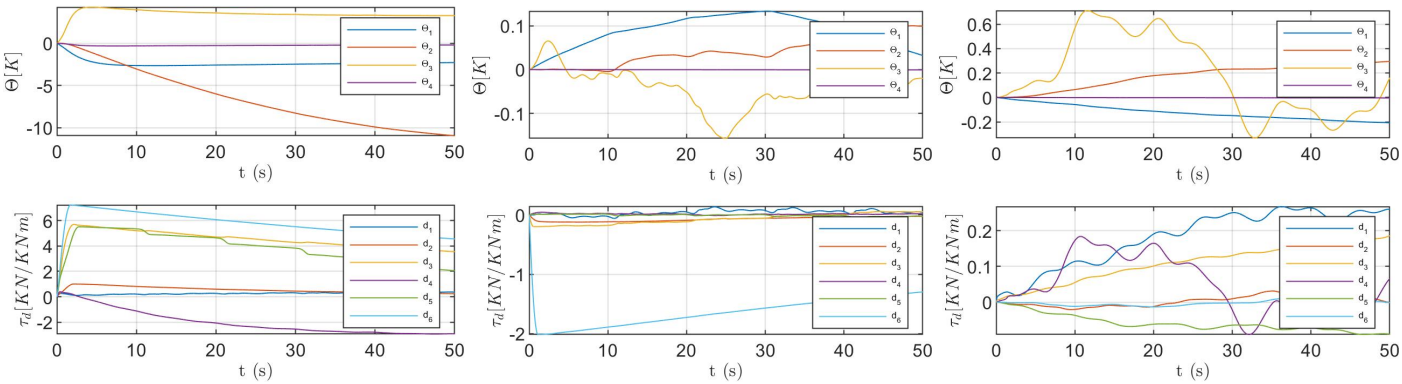


(**a**) Parameter history of Scenario 1. (**b**) Parameter history of Scenario 2. (**c**) Parameter history of Scenario 3.

**Figure 5.** Adaptive parameter history of Scenarios 1 to 3.

The tracking history of Scenario 2 is shown in Figure 6, and the related performance indices are given in Table 1. The adaptive parameter history of Scenario 2 is shown in Figure 5. The tracking performance of the PID controller is the worst in all directions, since the linear speed of the vehicle fluctuates within a certain range because of the time-varying ocean currents, as shown in Figure 6c,d, which in turn leads to the worst tracking performance. The attitude tracking performance indices $J_4$, $J_5$ and $J_6$ are the smallest, showcasing excellent accurate control performance. In addition, the heading angle of the vehicle reaches approximately 23 degrees fast and converges to 20 degrees slowly. Moreover, the vehicle reaches 23 degrees within 5 s, showcasing a short response time of the proposed controller, then converges to 20 degrees within 25 s, showcasing a stable tracking performance. The position tracking performance is also excellent. The position tracking errors $J_1$, $J_2$ and $J_3$ and the maximum tracking error $J_7$ of the proposed method are all the smallest. In this case, the initial system state errors are small and overestimation disappears, and the energy consumption of the proposed method is also the smallest. In this scenario, the performance indices of the proposed method are all the smallest, and the dynamic tracking performance of the proposed controller is verified.

**Table 1.** Controller performance comparison of the two scenarios.

| Scenario | Method | $J_1$ | $J_2$ | $J_3$ | $J_4$ | $J_5$ | $J_6$ | $J_7$ | $J_8$ |
|---|---|---|---|---|---|---|---|---|---|
| S1 | PID | 5.3 | 2.4 | 11.3 | 1.9 | 3.0 | 1.2 | \ | 286.3 |
| S1 | SMC | 6.2 | 2.2 | 5.6 | 0.7 | 1.8 | 0.9 | \ | 280.5 |
| S1 | Robust | 3.1 | 2.5 | 5.0 | 0.7 | 1.8 | 1.2 | \ | 217.8 |
| S1 | Proposed | 2.6 | 2.2 | 4.9 | 0.6 | 1.9 | 0.8 | \ | 266.4 |
| S2 | PID | 4.5 | 4.4 | 7.0 | 1.5 | 2.6 | 1.2 | 0.4 | 197.8 |
| S2 | SMC | 5.5 | 4.0 | 2.2 | 0.2 | 0.3 | 0.6 | 0.4 | 205.0 |
| S2 | Robust | 4.2 | 4.2 | 2.8 | 0.1 | 0.2 | 1.2 | 0.3 | 240.0 |
| S2 | Proposed | 2.6 | 3.3 | 0.7 | 0.1 | 0.1 | 0.5 | 0.2 | 176.9 |
| S3 | PID | 5.9 | 7.5 | 5.6 | 2.0 | 2.4 | 0.5 | \ | 125.6 |
| S3 | SMC | 5.3 | 6.9 | 4.5 | 0.8 | 0.3 | 0.02 | \ | 94.6 |
| S3 | Robust | 6.1 | 5.1 | 3.2 | 0.2 | 0.03 | 0.1 | \ | 171.6 |
| S3 | Proposed | 5.1 | 4.4 | 3.1 | 0.1 | 0.03 | 0.01 | \ | 174.2 |

\ means that no data is recorded.

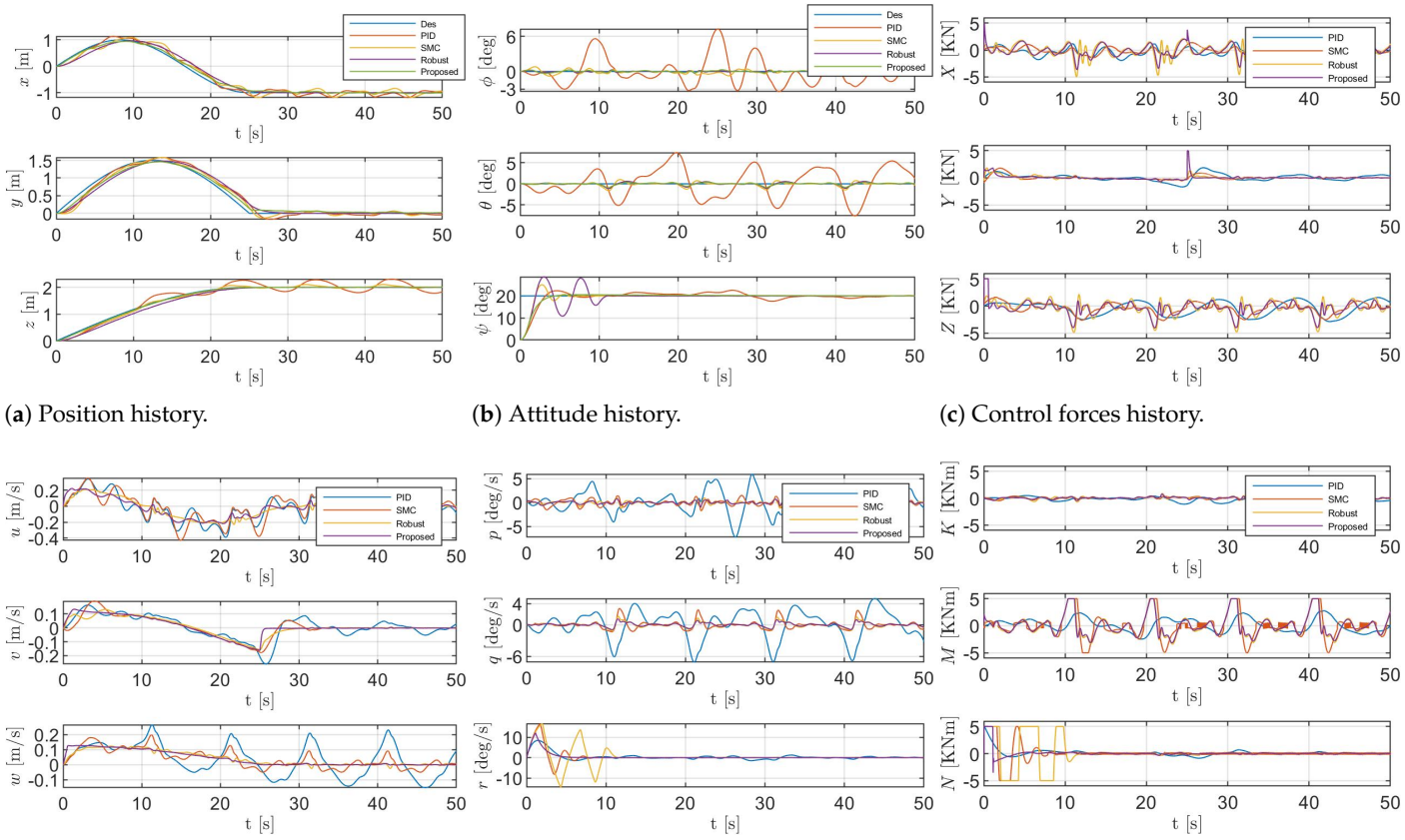


(**a**) Position history. (**b**) Attitude history. (**c**) Control forces history.

(**d**) Linear velocity history. (**e**) Angular velocity history. (**f**) Control torques history.

**Figure 6.** Tracking history of Scenario 2.

The tracking history of Scenario 3 is shown in Figure 7, and the related performance indices are given in Table 1. The adaptive parameter history of Scenario 3 is shown in Figure 5. This scenario is designed to verify the tip link tracking performance of the three controllers in intervention tasks. The tip link position tracking history is shown in Figure 7a. Notably, the inverse kinematics and the joint controller are the same in all the cases; thus, we conclude that the tip link tracking performance is highly related to the position and attitude control performance of the controller. The vehicle attitude control errors of the proposed method are the smallest; this, in turn, guarantees the tip link tracking performance. The tip link position tracking errors are also the smallest, with 5.1 ms in the surge direction, 4.4 ms in the sway direction and 3.1 ms in the heave direction. In this scenario, compared with the other three controllers, the tip link position tracking performance is the best, and the proposed controller is proven to enhance the precision of the tip link position control.

In these scenarios, the tracking performance of the proposed controller is better than those of the other controllers. The advantage of the proposed controller is the combination of the adaptive control law and the disturbance observer. The adaptive control law estimates the system buoyancy and changes in the COM and COB positions, and the disturbance observer estimates the external disturbances such as water currents. However, the adaptive problem, which is caused by the characteristics of the defined sliding surface, exists when the initial state errors are large and, in turn, introduce small tracking errors and stable tracking performance in the position and attitude. In real applications, stable attitude control of the system is actually more important than small errors. The onboard payload, such as a binocular camera, needs to obtain a precise measure with a stable attitude of the vehicle. Thus, the adaptive problem is acceptable. Moreover, the proposed controller has a short response time and good tracking performance, and it increases the intervention efficacy in real applications.

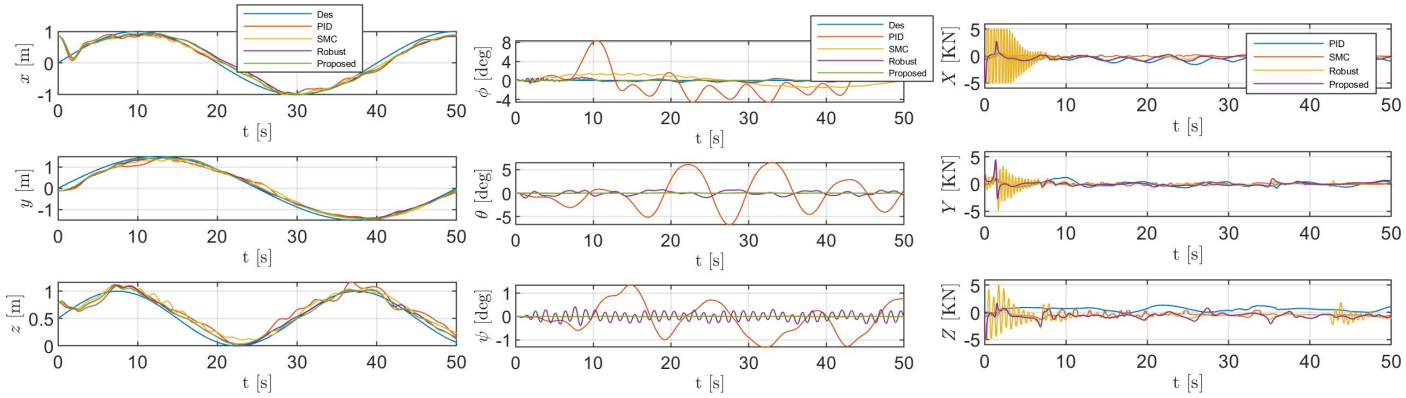


(**a**) Position history. (**b**) Attitude history. (**c**) Control forces history.

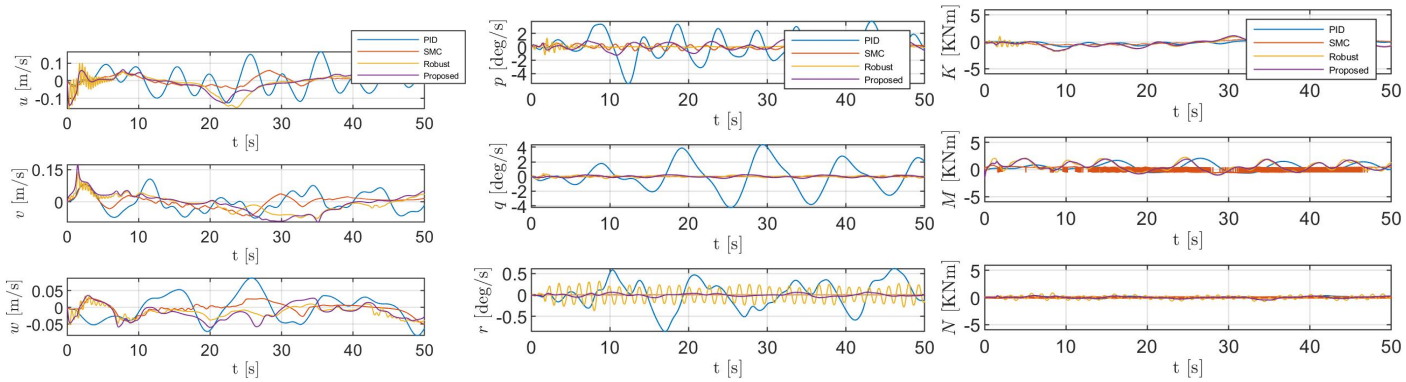


(**d**) Linear velocity history. (**e**) Angular velocity history. (**f**) Control torques history.

**Figure 7.** Tracking history of Scenario 3.

Parameter tuning of the proposed method is a skillful task for underwater manipulators systems, and the authors tune the parameters by the following steps. Firstly, choose the sliding surface gain $K_\Lambda$ to obtain a desired convergent performance of the stability, and large $K_\Lambda$ can decrease the position errors of the system. Then, choose $K_s$ based on the mass and inertia of the system to guarantee the response time of the system, and choose $K_\Theta$ and $\beta$ based on the speed of the manipulator to guarantee the convergent speed of the parameters. Finally, turn the parameters about the disturbance observer to compensate the external disturbances, and fine-tune $\beta$ to ensure the system stability. There is an estimation coupling problem of the adaptive law and disturbance observer. Thus, one should firstly tune the parameters of the adaptive law when the manipulator runs and then tune the parameters of the disturbance observer with disturbances.

On the basis of the above discussion, the proposed method is well suited to underwater intervention tasks for dynamic position tracking accuracy and stable attitude control performance, and we recommend that the proposed controller be applied together with measuring instruments and algorithms [27,28]. In addition, the proposed controller is suited to all kinds of underwater vehicles, since the adaptive law can estimate the COM and COB positions of the system and the disturbance observer can estimate the external disturbances. We record the time required for 100 calculations for the above four controllers: 7 ms, 11 ms, 7 ms and 16 ms for PID, SMC, Robust and Proposed controllers, respectively. The computation time of the proposed controller is about two times of that of the PID controller; however, the proposed controller can easily achieve high frequency in real applications.

The energy consumption is not considered in this work, while it is crucial for underwater systems. It will be optimized by combining optimal techniques in the future.

## 5. Conclusions

To realize precise control of UVMSs under coupling effects and external disturbances, we propose an adaptive controller with a nonlinear disturbance observer. The adaptive controller is designed to estimate the hydrostatic part of the coupling effects, and the nonlinear disturbance observer is designed to estimate the dynamic part of the coupling effects as well as external disturbances. A damping term is added to the adaptive law to attenuate the overestimation problem, and the stability of the proposed controller with parameter conditions is illustrated based on the basis of Lyapunov theory. Simulations are conducted via the MATLAB and Simurv platforms, and three scenarios are developed on the basis of the practical use of UVMSs. The simulation results show that the tracking errors of the proposed method in three scenarios are the smallest, showcasing the short response time and better tracking performance of the proposed method compared with those of the other three controllers.

We will conduct pool experiments to show the effectiveness of the proposed method in the real world.

**Author Contributions:** Methodology, X.Z., Y.W. and Q.T.; software, W.X. and G.W.; validation, X.Z. and Y.S.; investigation, X.Z.; resources, Q.Z. and X.W.; writing—original draft, X.Z.; writing—review and editing, X.Z., Y.W. and X.Y., supervision, Q.T. and Q.Z.; project administration, Q.Z.; funding acquisition, Q.T. and Q.Z. All authors have read and agreed to the published version of the manuscript.

**Funding:** This paper was supported by the Strategic Priority Research Program of the Chinese Academy of Sciences (Grant No. XDA22040102), Youth Innovation Promotion Association, Chinese Academy of Sciences (2023208) and fundamental research project of SIA.

**Institutional Review Board Statement:** Not applicable.

**Informed Consent Statement:** Not applicable.

**Data Availability Statement:** Readers can access our data by contacting the corresponding author.

**Acknowledgments:** The authors would like to thank the editors and reviewers related to this work.

**Conflicts of Interest:** The authors declare no conflicts of interest.

## References

1. Zheng, X.; Tian, Q.; Zhang, Q. Development and Control of an Innovative Underwater Vehicle Manipulator System. *J. Mar. Sci. Eng.* **2023**, *11*, 548. [CrossRef]
2. Zheng, X.H.; Wang, C.; Yang, X.J.; Tian, Q.Y.; Zhang, Q.F.; Zhai, B.Q. A Novel Thrust Allocation Method for Underwater Robots. In Proceedings of the 2022 12th International Conference on CYBER Technology in Automation, Control, and Intelligent Systems (CYBER), Changbai Mountain, China, 27–31 July 2022; pp. 271–276. [CrossRef]
3. Ribas, D.; Ridao, P.; Turetta, A.; Melchiorri, C.; Palli, G.; Fernández, J.J.; Sanz, P.J. I-AUV Mechatronics Integration for the TRIDENT FP7 Project. *IEEE/ASME Trans. Mechatronics* **2015**, *20*, 2583–2592. [CrossRef]
4. Qiyan, T.; Shuo, L.; Liying, Y.; Shiliang, S.; Bi, Z.; Yue, G.; Mei, S. Robots in Torch Relay at the Beijing 2022 Olympic and Paralympic Winter Games. *ROBOT* **2022**, *44*, 513–521. [CrossRef]
5. Yiqun, W.; Qiyan, T.; Yang, L.; Shuo, L.; Zhigang, L.; Qifen, Z.; Xinyu, L. The New Robots for Underwater Torch Relay at the Beijing 2022 Winter Olympic Games. *ROBOT* **2022**, *44*, 538–545. [CrossRef]
6. Borlaug, I.L.G.; Pettersen, K.Y.; Gravdahl, J.T. Combined kinematic and dynamic control of vehicle-manipulator systems. *Mechatronics* **2020**, *69*, 102380. [CrossRef]
7. Dai, Y.; Gao, H.; Yu, S.; Ju, Z. A fast tube model predictive control scheme based on sliding mode control for underwater vehicle-manipulator system. *Ocean Eng.* **2022**, *254*. [CrossRef]
8. Abbasi Moshaei, A.; Mohammadi Moghaddam, M.; Dehghan Neistanak, V. Analytical Model of Hand Phalanges Desired Trajectory for Rehabilitation and Design a Sliding Mode Controller Based on This Model. *Modares Mech. Eng.* **2020**, *20*, 129–137.
9. Han, L.; Tang, G.; Cheng, M.; Huang, H.; Xie, D. Adaptive Nonsingular Fast Terminal Sliding Mode Tracking Control for an Underwater Vehicle-Manipulator System with Extended State Observer. *J. Mar. Sci. Eng.* **2021**, *9*, 501. [CrossRef]
10. Li, M.; Yu, C.; Zhang, X.; Liu, C.; Lian, L. Fuzzy adaptive trajectory tracking control of work-class ROVs considering thruster dynamics. *Ocean Eng.* **2023**, *267*, 113232. [CrossRef]
11. Masmitja, I.; Martin, M.; O'Reilly, T.; Kieft, B.; Palomeras, N.; Navarro, J.; Katija, K. Dynamic robotic tracking of underwater targets using reinforcement learning. *Sci. Robot.* **2023**, *8*, eade7811. [CrossRef]

12. Tzeng, E.; Devin, C.; Hoffman, J.; Finn, C.; Peng, X.; Levine, S.; Saenko, K.; Darrell, T.J.A. Towards Adapting Deep Visuomotor Representations from Simulated to Real Environments. *arXiv* **2015**, arXiv:1511.07111.
13. Mohan, S.; Kim, J. Indirect adaptive control of an autonomous underwater vehicle-manipulator system for underwater manipulation tasks. *Ocean Eng.* **2012**, *54*, 233–243. [CrossRef]
14. Zhu, Q.; Shang, H.; Lu, X.; Chen, Y. Adaptive sliding mode tracking control of underwater vehicle-manipulator systems considering dynamic disturbance. *Ocean Eng.* **2024**, *291*, 116300. [CrossRef]
15. Yousefizadeh, S.; Bak, T. Unknown External Force Estimation and Collision Detection for a Cooperative Robot. *Robotica* **2019**, *38*, 1–17. [CrossRef]
16. Yang, Z.; Yan, Z.; Lu, Y.; Wang, W.; Yu, L.; Geng, Y. Double DOF Strategy for Continuous-Wave Pulse Generator Based on Extended Kalman Filter and Adaptive Linear Active Disturbance Rejection Control. *IEEE Trans. Power Electron.* **2022**, *37*, 1382–1393. [CrossRef]
17. Slotine, J.J.E.; Li, W. On the Adaptive Control of Robot Manipulators. *Int. J. Robot. Res.* **1987**, *6*, 49–59. [CrossRef]
18. Antonelli, G.; Caccavale, F.; Chiaverini, S.; Fusco, G. A novel adaptive control law for underwater vehicles. *IEEE Trans. Control Syst. Technol.* **2003**, *11*, 221–232. [CrossRef]
19. Wen-Hua, C. Disturbance observer based control for nonlinear systems. *IEEE/ASME Trans. Mechatronics* **2004**, *9*, 706–710. [CrossRef]
20. Yang, Y.; Du, J.; Liu, H.; Guo, C.; Abraham, A. A Trajectory Tracking Robust Controller of Surface Vessels With Disturbance Uncertainties. *IEEE Trans. Control Syst. Technol.* **2014**, *22*, 1511–1518. [CrossRef]
21. Fossen, T.I. Guidance and Control of Ocean Vehicles. 1999. Available online: https://api.semanticscholar.org/CorpusID:108605978 (accessed on).
22. Antonelli, G. Modelling of Underwater Robots. In *Underwater Robots*; Antonelli, G., Ed.; Springer International Publishing: Cham, Switzerland, 2014; pp. 23–63. [CrossRef]
23. Antonelli, G.; Chiaverini, S. Singularity-free regulation of underwater vehicle-manipulator systems. In Proceedings of the Proceedings of the American Control Conference, Toronto, ON, Canada, 8–12 July 2022; Volume 1, pp. 399–403. [CrossRef]
24. Antonelli, G.; Chiaverini, S.; Sarkar, N.; West, M. Adaptive control of an autonomous underwater vehicle: Experimental results on ODIN. *IEEE Trans. Control Syst. Technol.* **2001**, *9*, 756–765. [CrossRef]
25. Antonelli, G. Simurv 4.0. In *Underwater Robots*; Springer International Publishing: Cham, Switzerland, 2014; pp. 257–265. [CrossRef]
26. Healey, A.J.; Lienard, D. Multivariable sliding mode control for autonomous diving and steering of unmanned underwater vehicles. *IEEE J. Ocean. Eng.* **1993**, *18*, 327–339. [CrossRef]
27. Su, X.; Ullah, I.; Liu, X.; Choi, D. A Review of Underwater Localization Techniques, Algorithms, and Challenges. *J. Sens.* **2020**, *2020*, 6403161:1–6403161:24. [CrossRef]
28. Ullah, I.; Chen, J.; Su, X.; Esposito, C.; Choi, C. Localization and Detection of Targets in Underwater Wireless Sensor Using Distance and Angle Based Algorithms. *IEEE Access* **2019**, *7*, 45693–45704. [CrossRef]


**Disclaimer/Publisher's Note:** The statements, opinions and data contained in all publications are solely those of the individual author(s) and contributor(s) and not of MDPI and/or the editor(s). MDPI and/or the editor(s) disclaim responsibility for any injury to people or property resulting from any ideas, methods, instructions or products referred to in the content.